Available online at www.sciencedirect.com

SCIENCE DIRECT®

Journal of Photochemistry and Photobiology A: Chemistry 172 (2005) 322–330

Journal of Photochemistry and Photobiology A:Chemistry

www.elsevier.com/locate/jphotochem

Photochemistry of 4-(methylthio)phenylacetic acid
Steady-state and laser flash photolysis studies

Piotr Filipiak[a], Gordon L. Hug[b], Krzysztof Bobrowski[c], Bronislaw Marciniak[a,*]

[a] Faculty of Chemistry, Adam Mickiewicz University, 60-780 Poznan, Poland
[b] Radiation Laboratory, University of Notre Dame, Notre Dame, IN 46556, USA
[c] Institute of Nuclear Chemistry and Technology, Dorodna 16, 03-195 Warsaw, Poland

Received 25 September 2004; received in revised form 7 December 2004; accepted 20 December 2004

Abstract

The mechanism for the direct photolysis of 4-(methylthio)phenylacetic acid (4-MTPA) in acetonitrile was investigated using steady-state and laser flash photolysis. A variety of primary stable photoproducts was found under steady-state, 254 nm irradiation of acetonitrile solutions including carbon dioxide (photodecarboxylation), phenylacetic acid, dimethyl disulfide, methyl *p*-tolyl sulfide, 4-(methylthio)benzaldehyde, 4-(methylthio)benzyl alcohol and secondary stable photoproducts including toluene, benzyl alcohol, benzaldehyde, 1,2-diphenylethane. These stable photoproducts were identified and characterized using HPLC, GC, GC–MS, and UV–Vis methods. Quantum yields were determined for the formation of the various stable products in steady-state irradiations in the absence and in the presence of oxygen. Following laser flash photolysis (266 nm Nd:YAG laser) a variety of transients (e.g., the 4-MTPA triplet state and the sulfur-centered radical cation, $H_3C{-}S^{\bullet+}{-}C_6H_4{-}CH_2{-}COOH$) was found. A detailed mechanism of the primary and secondary processes is proposed and discussed. The photoinduced C–C bond cleavages are shown to result from an excited-singlet reaction pathway, and the C–S bond cleavages follow a triplet pathway. The validity of this proposed mechanism was supported by an analysis of the quantum yields of stable products and their transient precursors. The results from excited-state quenching by oxygen are also consistent with the proposed mechanism.

Keywords: 4-(Methylthio)phenylacetic acid; Photolysis; Bond cleavage; Radical; Quantum yield

1. Introduction

In recent years there has been interest in the nature of photolytic C–S bond cleavage, specifically whether it leads to radical-like or ionic products [1–3]. The conditions that determine which type of process occurs are of interest to synthetic organic chemists [1]. Furthermore, the relatively low ionization potential of sulfur centers in molecules make photoionization also a potential source of sulfur-centered radicals following photoexcitation. The source of photochemically generated sulfur radicals is the subject of the current work. The molecule chosen for investigation, 4-(methylthio)phenylacetic acid, has a C–C bond that is also photolabile and provides a standard against which to measure C–S bond cleavage.

Sulfur-centered free radicals and radical ions play important roles in diverse areas of chemistry. Sulfur compounds have found applications in industry for many decades [4], and sulfur-centered radicals are important intermediates in specialized organic synthesis [5–7]. Sulfur-centered radicals are also involved in atmospheric and environmental chemistry [8–10]. Their importance has been recognized in biological systems [11], for example, biological inactivation of peptides, proteins [12,13], hormones [14], and enzymes [15], oxidative stress [16], biological aging [17], pathologies such as Creutzfeldt–Jacob and Alzheimer's diseases [18,19], and radical repair mechanisms [20].

Recently sulfur-centered radicals, derived from aromatic carboxylic acids containing thioether groups, have been

---

* Corresponding author. Tel.: +48 61 829 1327; fax: +48 61 865 8008.
E-mail address: marcinia@amu.edu.pl (B. Marciniak).

1010-6030/$ – see front matter © 2004 Elsevier B.V. All rights reserved.
doi:10.1016/j.jphotochem.2004.12.022

shown to be effective when functioning as coinitiators in photopolymerization [21]. A tendency for sulfur radical cations to deprotonate [22] forming carbon-centered radicals situated adjacent to the sulfur atoms is significant for effective free-radical polymerization. Another mode of reactivity that is very important for initiating free-radical polymerization, is the decarboxylation of S-centered radicals derived from sulfur-containing carboxylic acids [21]. Most of the results published so far on sulfur-containing carboxylic acids concern the photochemistry of aliphatic sulfur-containing carboxylic acids. Sensitized photooxidation of various aromatic sulfur-containing carboxylic acids has been recently described [23]. In the present work, the mechanisms of direct photolysis of the sulfur-containing carboxylic acid, 4-(methylthio)phenylacetic acid (4-MTPA) are elucidated.

2. Experimental

2.1. Materials

4-(Methylthio)phenylacetic acid (4-MTPA), $p\text{-}H_3C\text{–}S\text{–}C_6H_4\text{–}CH_2\text{–}COOH$, was purchased both from Aldrich and Lancaster. 4-Carboxybenzophenone (CB) was from Aldrich. Methyl *p*-tolyl sulfide, $p\text{-}H_3C\text{–}S\text{–}C_6H_4\text{–}CH_3$; 4-(methylthio)benzaldehyde, $p\text{-}H_3C\text{–}S\text{–}C_6H_4\text{–}CHO$; 4-(methylthio)benzyl alcohol, $p\text{-}H_3C\text{–}S\text{–}C_6H_4\text{–}CH_2\text{–}OH$; dimethyl disulfide, $H_3C\text{–}S\text{–}S\text{–}CH_3$; and phenylacetic acid, $C_6H_5\text{–}CH_2\text{–}COOH$; were purchased from Aldrich. The deionized water for laser flash photolysis was purified in a reverse osmosis/deionization water system from Serv-A-Pure Co. Acetonitrile (for spectroscopy) was purchased both from Merck and J.T. Baker. All gases (C_2H_4, CO_2, H_2, He, Ar, N_2, O_2) were purchased both from BOC and Mittler Supply (South Bend, IN).

2.2. Steady-state photolysis: analysis of stable products and determination of quantum yields

Steady-state photolysis experiments were carried out in 1 cm × 1 cm rectangular UV cells on a standard optical-bench system. A low-pressure mercury lamp (Original Hanau TNN 15 W) was used as the excitation source for 254 nm irradiation. Solutions of 4-MTPA (4.55 mg) in acetonitrile (25 ml) were purged with high-purity argon (30 min) or oxygen (15 min) and then irradiated. Irradiated solutions were analyzed when the conversion of 4-MTPA was approximately 30% complete, i.e., 10–20 min of irradiation as monitored by high-pressure liquid chromatography (HPLC) analysis.

UV–Vis spectra were measured at room temperature using both a diode array spectrophotometer HP 8452A and a Cary 300 Bio Varian spectrophotometer.

The photolysis of 4-MTPA was monitored by HPLC using a Waters 600E Multisolvent Delivery System pump. The detection system consisted of a Waters 996 Photodiode Array UV–Vis Detector. Analytical HPLC was carried out on a Waters XTerra RP_{18} reverse phase column (4.6 mm × 250 mm, 5 μm particle size), eluent: phosphate buffer (70%)–acetonitrile (30%), flow rate: 1 ml/min, with optical detection at 210, 255, and 315 nm. HPLC–MS analyses were performed on this same system using a ZQ (electrospray) mass detector (Waters & Micromass).

Gas chromatographic (GC) analysis was performed on a Hewlett-Packard 5890 II series instrument equipped both with FID and TCD detectors in order to quantify CO_2 and also to identify stable products formed during steady-state photolysis. Analysis was done with both HP-HFAP and ULTRA 1 capillary columns (0.32 mm × 25 m) using a temperature program operating between 120 and 220 °C (heating rate, 10 °C/min) and a flow rate of 1.5 ml/min. GC–MS analysis was performed on a Varian Saturn 2100T instrument equipped with an ion trap. Analysis was done with a DB-5 capillary column (30 m).

The quantum yields, Φ were measured using uranyl oxylate actinometry at 254 nm taking its quantum yield to be 0.602 [24].

2.3. Laser flash photolysis

The nanosecond laser flash photolysis and its data acquisition system have been previously described in detail [25,26]. The Nd:YAG laser (PRO 230, Quanta-Ray Co.) provides 10–12 ns pulses. For the experiments described herein, the laser was operated at 266 nm and 10–12 mJ/pulse. The transients were monitored with a pulsed 1 kW xenon lamp, having the monitoring beam perpendicular to the laser beam. All experiments were carried out with a gravity-driven flow system and a rectangular quartz optical cell (0.5 cm × 1 cm). The monitoring-light pathlength was 0.5 cm. A solution of CB (2 mM) at neutral pH was used as a relative actinometer [27] by monitoring its triplet-triplet absorption ($\varepsilon_{535} = 6250\ M^{-1}cm^{-1}$) [28].

2.4. Pulse radiolysis

A Titan Beta model TBS 8/16-1S linear accelerator at the Notre Dame Radiation Laboratory provided 2–3 ns pulses of 8 MeV electrons [29], and the 10 MeV LAE 10 electron accelerator at the Institute of Nuclear Chemistry and Technology in Warsaw [30] provided 8 ns pulses. The data acquisition system allows for kinetic traces to be displayed on multiple time scales and has been described previously [31]. Absorbed doses per pulse were on the order of 6 Gy ($1\ Gy = 1\ J\ kg^{-1}$). Dosimetry was based on N_2O-saturated solutions containing 10^{-2} M KSCN, taking a radiation chemical yield of $G = 6.13$ radicals produced per 100 eV of absorbed energy ($0.635\ \mu M\ J^{-1}$) and a molar extinction coefficient of $7580\ M^{-1}\ cm^{-1}$ at 472 nm for the $(SCN)_2^{\bullet -}$ radical [32]. An absorbed dose of 6 Gy produces $[(SCN)_2^{\bullet -}] = 3.5\ \mu M$ in N_2O-saturated aqueous solutions based on $G = 6.13$.

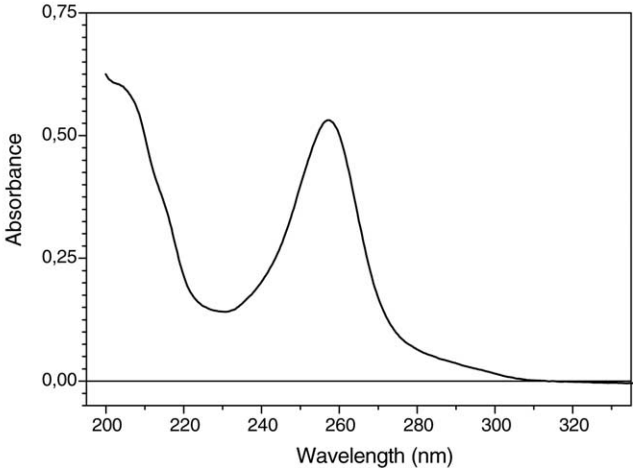

Fig. 1. UV–Vis absorption spectrum of 0.11 mM 4-MTPA in acetonitrile, taken in 1 cm × 1 cm UV cell, $\lambda_{max} = 257$ nm.

3. Results and discussion

3.1. Steady-state photolysis of 4-MTPA

The UV–Vis absorption spectrum presented in Fig. 1 is very similar to the spectrum of thioanisole [33]. Based on this similarity to thioanisole, the absorption band of 4-MTPA in the neighborhood 260 nm, can be attributed to a π–π^* transition [34].

Solutions of 4-MTPA in acetonitrile, were irradiated in the absence and presence of oxygen. The spectrophotometric changes were monitored by taking UV–Vis spectra at regular time intervals. The resulting spectra show the development of an absorption band between 200 and 240 nm (in the absence of oxygen) and the development of a new absorption peak at about 320 nm (in the presence of oxygen). These spectra also show a decrease in the absorption intensity at 257 nm, which reflects the decomposition of 4-MTPA.

GC–MS chromatography and HPLC were used for the identification of stable products formed during the direct steady-state photolysis of 4-MTPA. Oxygen-free acetonitrile solutions of 20 mM 4-MTPA were irradiated at 254 nm for 75 min and analyzed by GC–MS. A typical GC–MS chromatogram (Fig. 2a) shows a variety of primary and secondary stable photoproducts; these same products were detected in the HPLC analysis of the same irradiated solutions. The following main stable photoproducts were identified: phenylacetic acid, $C_6H_5{-}CH_2{-}COOH$; dimethyl disulfide, $H_3C{-}S{-}S{-}CH_3$; methyl *p*-tolyl sulfide, *p*-$H_3C{-}S{-}C_6H_4{-}CH_3$; CO_2; and $H_3C{-}S{-}C_6H_4{-}CH_2{-}CH_2{-}C_6H_4{-}S{-}CH_3$. On the other hand, when a similar analysis was performed on oxygen-saturated acetonitrile solutions of 4-MTPA, the resulting chromatograms showed different photoproducts (Fig. 2b) that appear in quite large concentrations following only 30 min of irradiation. The additional stable photoproducts that were identified in irradiated oxygen-saturated acetonitrile were

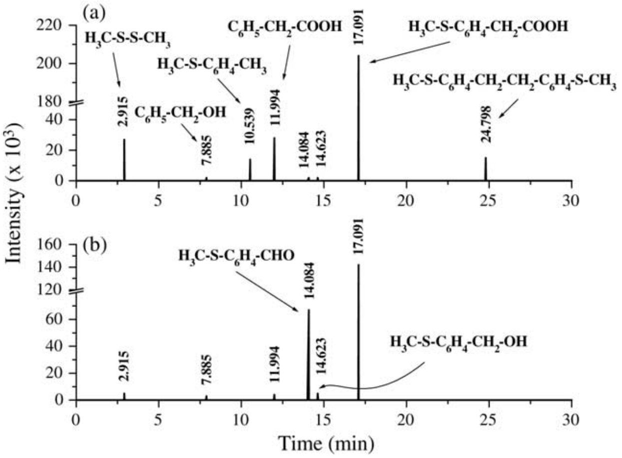

Fig. 2. (a) GC–MS chromatogram recorded after a 75 min irradiation of 4-MTPA (20 mM) in Ar-saturated acetonitrile. (b) GC–MS chromatogram recorded after a 30 min of irradiation of 4-MTPA (20 mM) in O_2-saturated acetonitrile.

4-(methylthio)benzaldehyde, *p*-$H_3C{-}S{-}C_6H_4{-}CHO$, and 4-(methylthio)benzyl alcohol, *p*-$H_3C{-}S{-}C_6H_4{-}CH_2{-}OH$. Supplementary gas chromatographic (GC) analyses were performed in order to identify CO_2 and to quantify its yield.

All of the primary and secondary stable photoproducts formed during the direct photolysis of 4-MTPA are shown in Scheme 1. The scheme is organized to indicate how the observed stable photoproducts were likely to form from competing and sequential bond cleavages. The presence of $C_6H_5{-}CH_2{-}COOH$ indicates that homolytic C–S bond cleavage is a primary photolytic process. By the same token the presence of *p*-$H_3C{-}S{-}C_6H_4{-}CH_3$ in the product mixture indicates that C–C bond cleavage is a competing primary photolytic process. Various observed products that are missing both the methylthio group and the acid group, i.e. toluene, indicate that secondary photolysis also occurred under our irradiation conditions. In the absence of oxygen, all the other observed products, except for CO_2, are free-radical combination products from the various radical fragments generated by the various C–S and C–C bond cleavages. The special products, mentioned above, that were observed in the presence of oxygen can be seen to arise following either via primary or secondary photolysis.

Since standard samples of the major products (vide supra), were commercially available, it was possible to determine their quantum yields by applying various chromatographic methods (mainly HPLC). The initial concentrations of 4-MTPA were varied from 1 to 5.4 mM in acetonitrile. The changes, Δc, in the concentrations of substrate and the various stable photoproducts were determined both by GC and HPLC measurements, using the authentic compounds as concentration standards. All quantum yields were extrapolated back to zero irradiation time or back-to-zero-percent conversion, in order to get the initial quantum yields. These procedures were necessary because of the absorption of the photolytic light by the photoproducts. Quantum yields de-

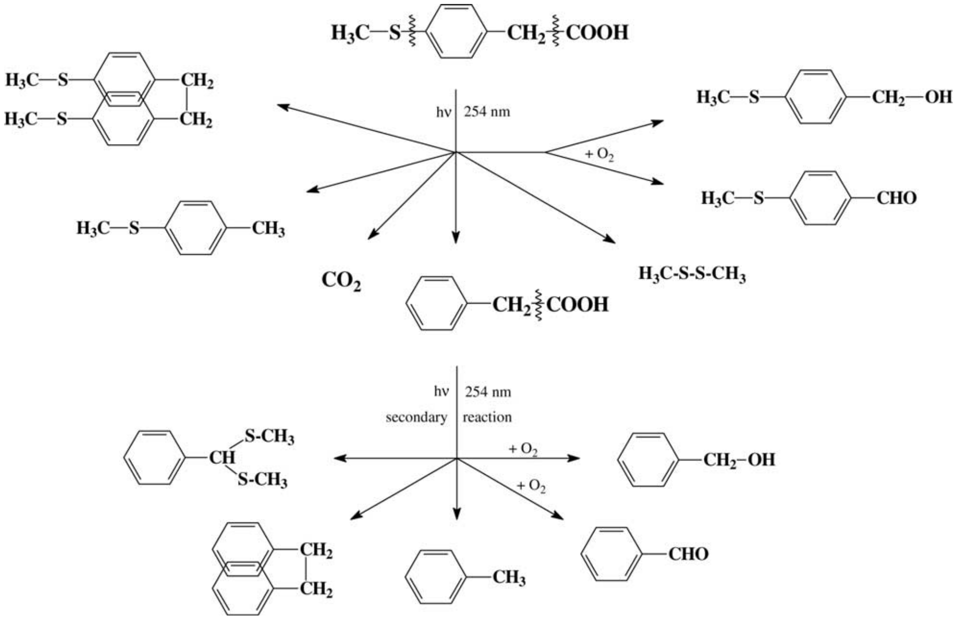

Scheme 1.

termined by these methods are presented in Table 1. It can be seen from Table 1 that, in the presence of oxygen, all the quantum yields (decomposition of substrate and formation of products) change significantly in comparison to the deaerated system. The participation of oxygen in the reaction mechanism is discussed below.

3.2. Pulse radiolysis—reference spectra

From the presence of formal C–C bond cleavage products ($H_3C{-}S{-}C_6H_4{-}CH_3$ and $H_3C{-}S{-}C_6H_4{-}CH_2{-}CH_2{-}C_6H_4{-}S{-}CH_3$), we anticipated that the C-centered radical, $^{\bullet}CH_2{-}C_6H_4{-}S{-}CH_3$, would be formed following the nanosecond laser flash photolysis of 4-MTPA. Previously, this radical was identified in the pulse radiolysis of 4-MTPA where it is formed following the decarboxylation of the sulfur-centered radical zwitterion, $H_3C{-}S^{\bullet+}{-}C_6H_4{-}CH_2{-}COO^-$. In order to characterize the spectral properties of these intermediates in detail, we used this same pulse radiolysis technique to generate these transients and to record their spectra. The pulse radiolysis of aqueous, N_2-saturated solutions containing 0.2 mM 4-MTPA, 2 mM $Na_2S_2O_8$, and 0.1 M *tert*-butanol (*t*-BuOH) at pH 5.5 yields a complex spectrum with absorption maxima at $\lambda_{max} = 270$, 320, and 560 nm. The reference spectra of the sulfur-centered radical zwitterions, $H_3C\text{-}S^{\bullet+}{-}C_6H_4{-}CH_2{-}COO^-$, and the C-centered radical, $^{\bullet}CH_2{-}C_6H_4{-}S{-}CH_3$, were obtained by resolution of the complex spectrum obtained in the pulse radiolysis experiment. The resolution procedure was described previously [23]. The analysis is a multivarient linear least squares regression [35]. The fitting parameters in the regression are the products of each transient's concentration multiplied by the optical pathlength of the monitoring light [36]. The data points, being fit, are the changes in optical density at each wavelength in the observed spectra at the time window in question. The other inputs to this procedure are the spectra (extinction coefficients) for each of the suspected transients. The reference spectrum (Fig. 3) of the sulfur-centered radical zwitterion, $H_3C{-}S^{\bullet+}{-}C_6H_4{-}CH_2{-}COO^-$ is an expanded spectrum compared to that shown previously [23]. This spectrum is characterized by two absorption max-

Table 1
Quantum yields for the decomposition of 4-(methylthio)phenylacetic acid and formation of primary photoproducts[a] in steady-state photolysis at 254 nm, and formation of 4-methylthiobenzyl radical[b] in laser flash photolysis at 266 nm in acetonitrile[c]

	4-MTPA	$C_6H_5CH_2{-}COOH$	$H_3CSC_6H_4{-}CH_2OH$	$H_3CSC_6H_4{-}CHO$	$H_3CSC_6H_4{-}CH_3$	H_3CSSCH_3[d]	$(H_3CSC_6H_4{-}CH_2)_2$	CO_2	$H_3CSC_6H_4{-}^{\bullet}CH_2$
$-O_2$	0.26	0.17	0.001	0.001	0.04	−0.07	0.03	0.04	−0.14
$+O_2$	0.09	0.002	0.005	0.07	≤0.001	−0.002	≤0.001	–[e]	–

[a] From steady-state measurements, extrapolated to zero-percent conversion of 4-MTPA, estimated errors ± 10%.
[b] From laser flash photolysis, estimated values with errors ± 20% (see text) {[4-MTPA] = 60 μM}.
[c] [4-MTPA] = 1.0–20.3 mM, $I_0 = (2.07\text{–}4.35) \times 10^{-4}$ einstein dm^{-3} min^{-1}.
[d] Estimated error ± 20%.
[e] Not determined.

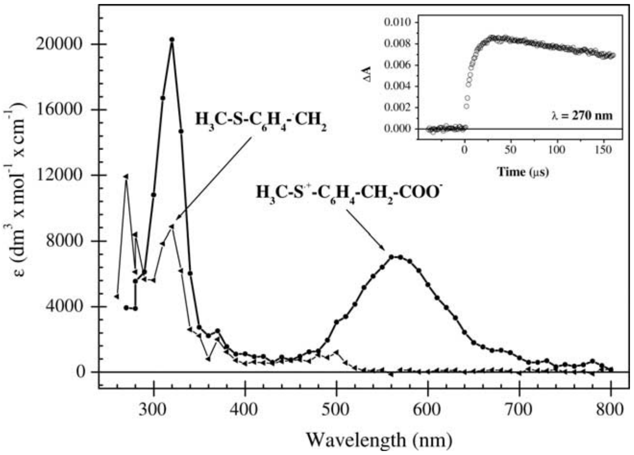

Fig. 3. Reference spectra of (i) $CH_3S^{\bullet+}—C_6H_4—CH_2—CO_2^-$: $\varepsilon_{560} = 7000\,M^{-1}\,cm^{-1}$, recorded 2–3 μs following pulse radiolysis of an N_2-saturated aqueous solution (see text and [23]), and (ii) $H_3C—S—C_6H_4—^{\bullet}CH_2$: $\varepsilon_{500} = 1200\,M^{-1}\,cm^{-1}$, recorded 110 μs following pulse radiolysis of an N_2-saturated aqueous solution, pH 5.5, for 0.2 mM $CH_3—SC_6H_4—CH_2—COO^-$ (**3**), 2 mM $Na_2S_2O_8$, and 0.1 M *t*-BuOH. Inset shows experimental trace for decay of $H_3C—S—C_6H_4—^{\bullet}CH_2$ taken at 270 nm.

ima located at $\lambda_{max} = 320$ and 560 nm with the respective molar extinction coefficients ($\varepsilon_{320} = 20{,}300\,M^{-1}\,cm^{-1}$ and $\varepsilon_{560} = 7000\,M^{-1}\,cm^{-1}$) [23].

The reference spectrum of the C-centered radical, $^{\bullet}CH_2–C_6H_4–S–CH_3$ (Fig. 3) is characterized by three absorption maxima located at $\lambda_{max} = 270$, 320, and 500 nm with the respective molar extinction coefficient ($\varepsilon_{270} = 11{,}900\,M^{-1}\,cm^{-1}$, $\varepsilon_{320} = 8900\,M^{-1}\,cm^{-1}$, and $\varepsilon_{500} = 1200\,M^{-1}\,cm^{-1}$).

3.3. Nanosecond laser flash photolysis of 4-MTPA

Solutions of 60 μM 4-MTPA in acetonitrile were irradiated with 10 ns pulses from the fourth harmonic (266 nm) of a Nd:YAG laser. Transient absorption was seen in the region of 280–700 nm in argon-saturated solutions, see Fig. 4. The transient spectra shown in Fig. 4 were assembled from kinetic traces and displayed at a few selected time delays (between 60 ns and 60 μs) following the laser pulse. Inset (a) in Fig. 4 shows a 390 nm kinetic trace on an expanded time scale. This kinetic trace can be fit to an exponential decay with a rate constant of $8.6 \times 10^5\,s^{-1}$ or a lifetime of 1.1 μs. The transient signal is assigned to the decay of the triplet state of 4-MTPA, see below. On the same time scale, the kinetic trace at 560 nm (inset 4b) shows a decay with a rate constant equal to $2.6 \times 10^5\,s^{-1}$ or a lifetime of 3.8 μs which is different from that recorded at 390 nm. These observations indicate that there are at least two different transient species present in the solution. Spectral resolution of the transient spectra into components (based on reference spectra obtained in pulse radiolysis [23]) was used in the identification of these intermediate products.

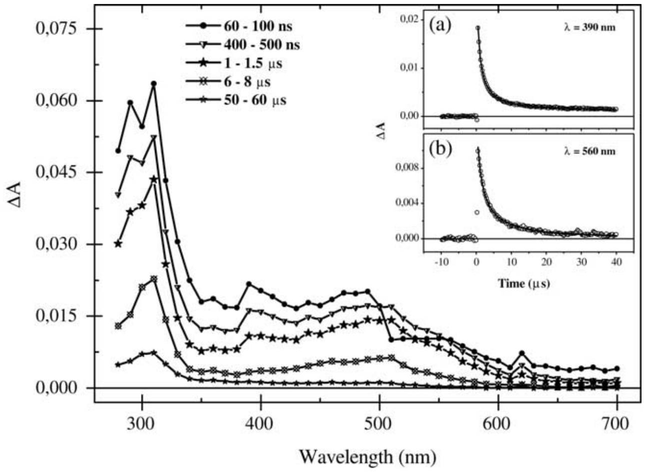

Fig. 4. Transient absorption spectra following 266 nm laser flash photolysis of $H_3C—S—C_6H_4—CH_2—COOH$ (4-MTPA) (60 μM), in Ar-saturated acetonitrile, recorded at five different delay times, relative actinometry: [*T*] = 23.4 μM. Inset shows experimental trace for decays taken at 390 nm ((a) triplet state of 4-MTPA) and 560 nm ((b) sulfur-centered radical cation).

A significant contribution to the transient spectra shown in Fig. 4, is due to the spectrum of the triplet state of 4-MTPA. The triplet-state spectrum is characterized by a broad absorption band covering almost the whole of the accessible spectral region (280–650 nm), with an absorption maximum around 390 nm. This spectral assignment to the triplet state is based on a comparison of the transient absorption spectra in the absence (Fig. 4) and presence (Fig. 5) of oxygen. The spectra shown in Fig. 5 (for the oxygen-saturated solution) are generated from kinetic traces and displayed at several selected time delays (between 40 ns and 60 μs) following the laser pulse. Inset (a) in Fig. 5 shows a 390 nm kinetic trace that represents the decay of the triplet state

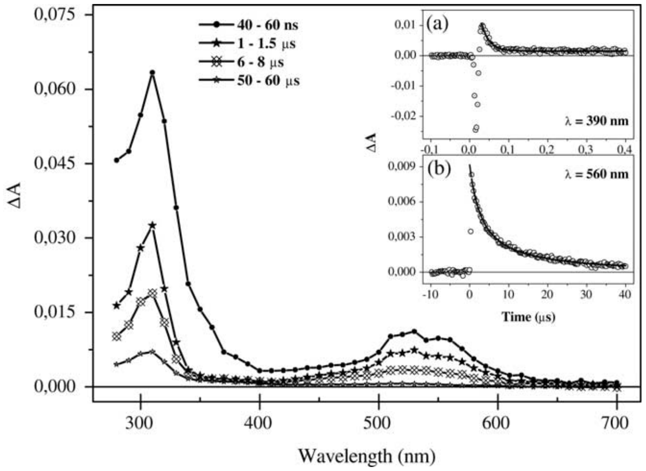

Fig. 5. Transient absorption spectra following 266 nm laser flash photolysis of $H_3C—S—C_6H_4—CH_2—COOH$ (4-MTPA) (60 μM), in O_2-saturated acetonitrile, recorded at four different delays times, relative actinometry: [*T*] = 23.4 μM. Inset shows experimental trace for decays taken at 390 nm ((a) triplet state of 4-MTPA) and 560 nm ((b) sulfur-centered radical cation).

of 4-MTPA on an expanded time scale. In the presence of oxygen, the 390 nm transient decays with a rate constant of $6.2 \times 10^7\ s^{-1}$or a lifetime of 16 ns. This enhanced decay in the presence of oxygen can be explained as being due to the rapid quenching of the triplet state of 4-MTPA by oxygen ($k_q \sim 7 \times 10^9\ M^{-1}\ s^{-1}$, based on the two pseudo-first order decay constants).

The kinetic trace at 560 nm for the sulfur-centered radical cation (inset 5b) shows a decay with a rate constant of $2.6 \times 10^5\ s^{-1}$ or a lifetime of 3.8 μs. This intermediate species was assigned following spectral resolutions into component spectra using reference spectra obtained from pulse radiolysis [23]. We did not observe any faster decay of the 560 nm absorption band when oxygen was present. This is consistent with the assignment of the 560 nm band being due to the sulfur-centered radical cation because such radicals normally have small rate constants for their reactions with oxygen [37].

We could not accurately resolve the spectra of the various C-centered radicals since their absorption spectra clustered at the edge of our effective spectral window of observation which was limited by the absorption of the substrate itself. For instance, the absorption spectrum the phenyl radical of phenylacetic acid is expected to be below 300 nm resembling phenylacetic acid itself. Phenyl radicals tend to resemble their parent compounds [38,39]; presumably the unpaired electron being in a σ orbital minimally effects the π system. This difficulty (narrowness of the spectral window) did not allow us to sample a wide enough range of wavelengths to accomplish a reliable spectral resolution. Therefore it was only possible to estimate the quantum yields of the remaining transients taking changes in transient absorbances at appropriate wavelengths in the presence or absence of oxygen. All quantum yields were extrapolated back to time zero (end of laser pulse) in order to ascertain the initial quantum yields.

One quantum yield so estimated by this method is presented in the last column of Table 1. In spite of the limitations described above, it can be seen from Table 1 that the quantum yield for the formation of $H_3C{-}S{-}C_6H_4{-}{}^{\bullet}CH_2$ radicals (≈0.14) is roughly the same as the sum of the steady-state quantum yields (0.04) for the formation of *p*-$H_3C{-}S{-}C_6H_4{-}CH_3$ and twice (0.03) for the formation of $H_3C{-}S{-}C_6H_4{-}CH_2{-}CH_2{-}C_6H_4{-}S{-}CH_3$. These are all the observed primary photoproducts that can be formed from the $H_3C{-}S{-}C_6H_4{-}{}^{\bullet}CH_2$ radical. Thus there is a correspondence between quantum yields determined separately by steady-state and laser flash photolysis, and they match within experimental error. Further rationalization for the discrepancy is given below.

It can be seen from the values in Table 1 that the presence of oxygen significantly changes the quantum yields (i.e., the decomposition of the substrate from steady-state analysis and also the formation of the transients). As discussed below, these oxygen effects give critical clues to the mechanism of direct photolysis.

3.4. Mechanism

Even a cursory examination of the primary photoproducts and their quantum yields in Table 1 reveals two striking generalizations. First the photoproducts fall into two groups each of which is derived from a formal bond cleavage (C–S versus C–C). Second, in the presence of oxygen, the photoproducts are predominately from the group derived from a formal C–C bond cleavage. The effect of oxygen on the transient absorptions was already used (see above) to assign the 390 nm transient to the triplet state of 4-MTPA. Therefore, if the phenomena of triplet-state quenching by oxygen is juxtaposed with the lack of C–S bond cleavage in the presence of oxygen, it is reasonable to conclude that the C–S bond cleavage in 4-MTPA is all, or in large part, a triplet-state reaction. By elimination, the C–C bond-cleavage products (in particular, $H_3C{-}S{-}C_6H_4{-}CHO$) that remain in the presence of oxygen are likely formed via an excited-singlet pathway.

Based on the hypothesis that these pathways are independent, a mechanism (Scheme 2) for the direct photolysis of 4-MTPA is proposed. The following examination of the quantitative results shows that this hypothesis holds to a large extent. Overall, the 4-MPTA decomposition quantum yield of 0.26 is broken down into 0.17 going into $C_6H_5{-}CH_2{-}COOH$ (via the triplet pathway) and 0.09 which still decomposes via the single pathway when oxygen is present. The 74% of the photons not leading to decomposition of 4-MTPA (in the absence of oxygen) can be partitioned into radiationless transitions, either internal conversion (IC) from the excited-singlet state or intersystem crossing (ISC) from the triplet to the ground state. From the data we do not know how the radiationless transitions are partitioned into these two pathways. The value of 0.17 is the product of the quantum yield of triplet formation times the probability that C–S bond cleavage occurs in the triplet state.

Examination of the quantum yields associated with the singlet mechanism demonstrates that the measured yields are largely consistent with the proposed Scheme 2. The quantum yield of 0.09 from the decomposition of 4-MTPA in the presence of oxygen should occur whether or not oxygen is present if the mechanism is due to photochemistry from a relatively short-lived singlet state which is minimally quenched by oxygen. The values in the absence of oxygen are consistent with this. In particular, one of the main products is $H_3C{-}S{-}C_6H_4{-}CH_2{-}CH_2{-}C_6H_4{-}S{-}CH_3$ which is formed with a quantum yield of 0.03. However, since it is formed by combination of two $H_3C{-}S{-}C_6H_4{-}{}^{\bullet}CH_2$ radicals, this product accounts for $2 \times 0.03 = 0.06$ of the 0.09 quantum yield. The additional quantum yield (0.04) for the formation of *p*-$H_3C{-}S{-}C_6H_4{-}CH_3$ accounts for the rest of the quantum yield of the singlet degradation of 4-MTPA in the absence of oxygen, as least within experimental error. When oxygen is present, the quantum yields of 0.07 for aldehyde formation and 0.005 for alcohol formation is, within experimental error, the quantum yield of 4-MTPA degradation (0.09) in the presence of oxygen.

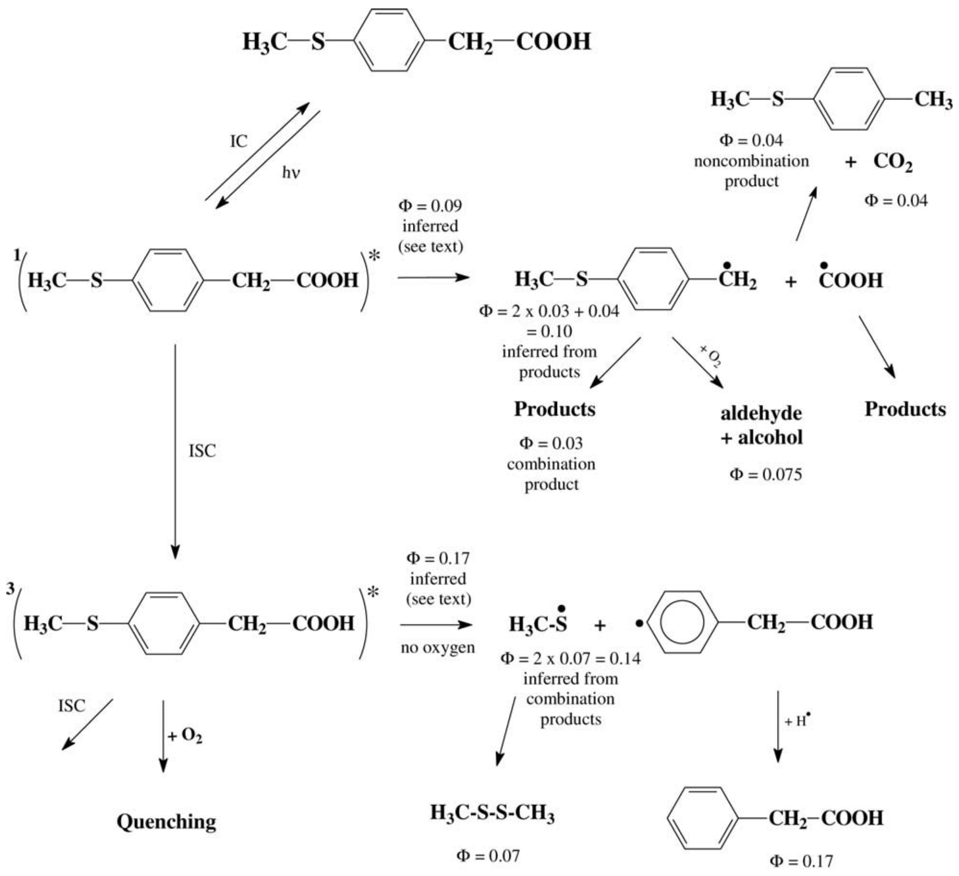

Scheme 2.

The second reaction pathway, i.e. that occurring through the excited triplet state, involves a homolytic C–S bond cleavage. It leads to formation of the *p*-carboxymethylenephenyl radical, $^{\bullet}C_6H_5{-}CH_2{-}COOH$, and by implication its complementary product the methylthiyl radical, $H_3C{-}S^{\bullet}$. In the absence of oxygen, the quantum yield of 0.17 for the formation of $C_6H_5{-}CH_2{-}COOH$ is consistent with the difference in the quantum yields of 4-MTPA degradation in the absence and the presence of oxygen. The other primary product that suggests C–S fragmentation, i.e. $H_3C{-}S{-}S{-}CH_3$, must come from two C–S fragmentations and thus contributes $2 \times 0.07 = 0.14$ which matches the quantum yield (0.17) for its complementary product, i.e., $C_6H_5{-}CH_2{-}COOH$. On the other hand, when oxygen is present, the triplet pathway is inhibited by efficient triplet-state quenching by oxygen ($k_q \sim 7 \times 10^9\ M^{-1}\ s^{-1}$, see above). In the presence of oxygen, little or no steady-state products can be ascribed as being formed from the two radicals ($^{\bullet}C_6H_5{-}CH_2{-}COOH$ and $H_3C{-}S^{\bullet}$) from homolytic C–S bond cleavages.

The plausibility of the triplet mechanism can be checked by calculating k_q from the Stern–Volmer equation

$$\frac{\Phi_p^0}{\Phi_p} = 1 + \tau_T k_q [O_2] \qquad (1)$$

where Φ_p^0 and Φ_p are the quantum yields of phenylacetic acid formation in the absence and presence of oxygen, respectively. The concentration of oxygen is 9.1 mM in acetonitrile [40], and the triplet lifetime, τ_T, in argon-saturated solutions was measured to be 1.1 μs, see above. The resulting k_q from Eq. (1) is $\sim 8 \times 10^9\ M^{-1}\ s^{-1}$. The agreement between the k_q values from the O_2 quenching of the triplet absorption and the O_2 quenching of the phenylacetic acid quantum yields supports the assertion that the homolytic C–S bond cleavage arises from the triplet-reaction pathway.

Another possible process needs to be considered when large numbers of photons are present. In the laser flash photolysis experiments, there is the possibility that biphotonic, or multiphotonic, absorption can lead to the formation of the sulfur-centered radical cation, $H_3C{-}S^{\bullet+}{-}C_6H_4{-}CH_2{-}COOH$. This radical is actually observed in transient spectra following laser flash photolysis. This sulfur-centered radical cation can decay by at least two processes. One of them is deprotonation, and the other is decarboxylation which occurs by C–C bond cleavage leading to the 4-methylthiobenzyl radical, $H_3C{-}S{-}C_6H_4{-}^{\bullet}CH_2$. The production of these extra multiphotonically generated radicals is why, the quantum yield for formation of this radical ($\Phi \sim 0.14$) via laser flash photolysis is higher than sum of quantum yields for formation of steady-state products formed from this radical ($\Phi \sim 0.10$). Unfortunately we do not have a good estimate of the laser-induced quantum yield of the 4-methylthiobenzyl radical, $H_3C–S–C_6H_4–{}^{\bullet}CH_2$, formed by this pathway in acetonitrile (i.e., from the sulfur-centered radical cation). Such a multiphotonic process is not possible under our steady-state photolysis conditions because of low probability of two-photon absorption. Thus, in Scheme 2, we do not show processes involving sulfur-centered radical cations.

What carboxyl fragment results from the C–C bond cleavage depends on the state of protonation of 4-MTPA and the nature of the cleavage itself. In acetonitrile, 4-MTPA almost certainly exists in its protonated form. This supposition is based on the expectation that the pK_a of 4-MTPA in acetonitrile is approximately the same as those of benzoic acid [41] and acetic acid [42] which have pK_a values of 20.7 and 22.3, respectively, in acetonitrile. The C–C bond cleavage in Scheme 2 is shown as being homolytic. This is based on the analogy with phenylacetic acid that has been ascertained [43,44], after some controversy, as being homolytic in some common nonaqueous solvents. The $HOC^{\bullet}O$ radical would be formally the result of such a homolytic bond cleavage of the protonated form of the acid. The $HOC^{\bullet}O$ radical is known in gas phase work [45].

The one quantum yield that has not yet been discussed is that of CO_2. Its quantum yield (0.04 in the absence of oxygen) does match the quantum yield of $H_3C–S–C_6H_4–CH_3$ which might indicate that CO_2 is formed in a geminate reaction of the pairs of radicals formed from the C–C bond cleavage. The geminate reaction would not involve the reforming of the C–C bond but would involve an H-abstraction yielding CO_2 and the stable molecule, $H_3C–S–C_6H_4–CH_3$. However, this accounts for only half of the $HOC^{\bullet}O$ radicals that should be formed (0.09). No irradiation products related to $HOC^{\bullet}O$ other than CO_2 were found as stable compounds.

Acknowledgments

This work was supported by the Committee for Scientific Research, Poland (Grant 3TO 9A 03719), by the European Community's Human Potential Program under Contract HPRN-CT-2002-00184 (SULFRAD) and by the Office of Basic Energy Sciences of the U.S. Department of Energy (GLH). This paper is Document No. NDRL 4553 from the Notre Dame Radiation Laboratory.

References

[1] P.J. Kropp, G.E. Fryxell, M.W. Tubergen, M.W. Hager, G.D. Harris Jr., T.P. McDermott Jr., R. Tornero-Velez, J. Am. Chem. Soc. 113 (1991) 7300.
[2] S.A. Fleming, A.W. Jensen, J. Org. Chem. 61 (1996) 7040.
[3] D. Vialaton, C. Richard, J. Photochem. Photobiol. A: Chem. 136 (2000) 169.
[4] E.E. Reid, Organic Chemistry of Bivalent Sulfur, Chemical Publishing, New York, 1958.
[5] A. Wrzyszczynski, F. Scigalski, J. Paczkowski, Nukleonika 45 (2000) 73.
[6] C. Chatgilialoglu, M.P. Bertrand, C. Ferreri, Sulfur-centered radicals in organic synthesis, in: Z.B. Alfasi (Ed.), S-centered Radicals, Wiley, Chichester, 1999, pp. 311–354.
[7] N.L. Bauld, J.T. Aplin, W. Yueh, A. Loinaz, J. Am. Chem. Soc. 119 (1997) 11381.
[8] R.P. Wayne, Chemistry of Atmospheres, 2nd ed., Clarendon Press, Oxford, 1991.
[9] T. Tobien, W.J. Cooper, M.G. Nickelsen, E. Pernas, K.E. O'Shea, K.-D. Asmus, Environ. Sci. Technol. 34 (2000) 1286.
[10] S.P. Urbanski, P.H. Wine, Chemistry of gas phase sulfur-centered radicals, in: Z.B. Alfasi (Ed.), S-centered Radicals, Wiley, Chichester, 1999, pp. 97–140.
[11] M. Friedman, The Chemistry and Biochemistry of the Sulhydryl Group in Amino Acids, Peptides and Proteins, Pergamon Press, New York, 1973.
[12] N. Brot, H. Weissbach, Arch. Biochem. Biophys. 223 (1983) 271.
[13] W. Vogt, Free Radical. Biol. Med. 18 (1995) 93.
[14] L.-C. Teh, L.J. Murphy, N.L. Huq, J. Biol. Chem. 262 (1987) 6472.
[15] D. Johnson, J. Travis, J. Biol. Chem. 254 (1979) 4022.
[16] P. Wardman, Thiyl radicals in biology: their role as a 'molecular switch' central to cellular oxidative stress, in: Z.B. Alfasi (Ed.), S-centered Radicals, Wiley, Chichester, 1999, pp. 289–309.
[17] B. Barlett, E.R. Stadtman, J. Biol. Chem. 272 (1997) 20313.
[18] C. Schöneich, Exp. Gerontol. 34 (1999) 19.
[19] W.R. Markesbery, Free Radical. Biol. Med. 23 (1997) 134.
[20] C. Chatgilialoglu, K.-D. Asmus, Sulfur-centered Reactive Intermediates in Chemistry and Biology, Plenum Press, New York, 1989.
[21] A. Wrzyszczynski, P. Filipiak, G.L. Hug, B. Marciniak, J. Paczkowski, Macromolecules 33 (2000) 1577.
[22] J. Mönig, R. Goslich, K.-D. Asmus, Ber. Bunsenges. Phys. Chem. 90 (1986) 115.
[23] P. Filipiak, G.L. Hug, I. Carmichael, A. Korzeniowska-Sobczuk, K. Bobrowski, B. Marciniak, J. Phys. Chem. A 108 (2004) 6503.
[24] S.L. Murov, I. Carmichael, G.L. Hug, Handbook of Photochemistry, Marcel Dekker, New York, NY, 1993, 124 pp.
[25] M.D. Thomas, G.L. Hug, Comput. Chem. (Oxford) 22 (1998) 491.
[26] V. Nagarajan, R.W. Fessenden, J. Phys. Chem. 89 (1985) 2330.
[27] I. Carmichael, G.L. Hug, J. Phys. Chem. Ref. Data 15 (1986) 1.
[28] J.K. Hurley, H. Linschitz, A. Treinin, J. Phys. Chem. 92 (1988) 5151.
[29] K. Whitham, S. Lyons, R. Miller, D. Nett, P. Treas, A. Zante, R.W. Fessenden, M.D. Thomas, Y. Wang, Linear accelerator for radiation chemistry research at Notre Dame, in: Particle Accelerator Conference and International Conference on High Energy Accelerators, Dallas, TX, USA, 1995.
[30] J. Mirkowski, P. Wisniowski, K. Bobrowski, INCT Annual Report 2000, Institute of Nuclear Chemistry and Technology, 2000.
[31] G.L. Hug, Y. Wang, C. Schöneich, P.-Y. Jiang, R.W. Fessenden, Radiat. Phys. Chem. 54 (1999) 559.
[32] E. Janata, R.H. Schuler, J. Phys. Chem. 86 (1982) 2078.
[33] , UV Atlas of Organic Compounds, vol. IV, Butterworths, London, 1968, D8/8 pp.
[34] C.N.R. Rao, Ultra-violet and visible spectroscopy, in: Chemical Applications, Butterworths, London, 1975, 81 pp.
[35] P.R. Bevington, Data Reduction and Error Analysis for the Physical Sciences, McGraw-Hill, New York, 1969.
[36] B. Marciniak, K. Bobrowski, G.L. Hug, J. Phys. Chem. 97 (1993) 11937.
[37] N.P. Schepp, L.J. Johnston, J. Am. Chem. Soc. 116 (1994) 6895.
[38] B. Cercek, M. Kongshaug, J. Phys. Chem. 74 (1970) 4319.
[39] J.G. Radziszewski, Chem. Phys. Lett. 301 (1999) 565.
[40] W.D.K. Clark, C. Steel, J. Am. Chem. Soc. 93 (1971) 6347.

[41] J.F. Coetzee, Ionic reactions in acetonitrile, in: A. Streitwieser Jr., R.W. Taft (Eds.), Progress in Physical Organic Chemistry, vol. 4, Interscience, New York, 1967, pp. 45–92.
[42] I.M. Kolthoff, M.K. Chantooni Jr., S. Bhowmik, J. Am. Chem. Soc. 90 (1968) 23.
[43] G.A. Epling, A. Lopes, J. Am. Chem. Soc. 99 (1977) 2700.
[44] D. Budac, P. Wan, J. Photochem. Photobiol. A: Chem. 67 (1992) 135.
[45] I. Carmichael, J. Phys. Chem. 98 (1994) 5896.